Origin and dynamics of mesoscale eddies in the Catalan Sea (NW Mediterranean): Insight from a numerical model study

A. Rubio, B. Barnier, G. Jorda, M. Espino, Patrick Marsaleix

Origin and dynamics of mesoscale eddies in the Catalan Sea (NW Mediterranean): Insight from a numerical model study

A. Rubio,[1,2] B. Barnier,[3] G. Jordà,[4] M. Espino,[1] and P. Marsaleix[5]

Received 26 March 2007; revised 27 November 2008; accepted 23 March 2009; published 9 June 2009.

[1] Past observations and satellite sea surface temperature imagery indicate the presence of mesoscale anticyclonic eddies drifting along the Catalan coast. In September 2001 one of these anticyclonic eddies was surveyed over the shelf break during an oceanographic cruise which permitted the 3-D description of its structure. In this work we investigate the origin and dynamics of such "Catalan eddies" using a numerical circulation model of the northwest Mediterranean at 3 km resolution driven by high-resolution atmospheric analyses and compare model eddies with the observations in the Catalan Sea. We identify two zones of eddy formation in the Gulf of Lions, in front of the city of Marseille and at the southeast of coast of Roussillon, from which anticyclonic eddies are observed to drift toward the Catalan Sea. The hydrology and dynamics of the structures observed in the simulations are characterized. Sensitivity experiments and energy analysis are performed which allow us to identify the mechanisms associated with their generation. Properties of the eddy observed during the 2001 cruise at the Catalan shelf break are found to compare well with model eddies generated at the southeast of the Roussillon coast. The model relates the origin of these eddies to the separation of the coastal current downstream from Creus Cape: flow separation is linked to intense downwelling taking place in front of the Roussillon coast when strong northwesterly winds events occur.

Citation: Rubio, A., B. Barnier, G. Jordà, M. Espino, and P. Marsaleix (2009), Origin and dynamics of mesoscale eddies in the Catalan Sea (NW Mediterranean): Insight from a numerical model study, *J. Geophys. Res.*, *114*, C06009, doi:10.1029/2007JC004245.

1. Introduction

[2] In the NW Mediterranean (Figure 1), the Northern Current (hereinafter referred to as NC) flows from the Ligurian to the Catalan Sea following the continental slope (1000–2000 meters isobaths) and leaving low-salinity shelf waters at its coastal side [*Astraldi et al.*, 1990]. This current is about 30–50 km wide and 300–400 m deep, has maximum surface velocities between 0.3 and 0.5 m s^{-1} and an associated volume transport of 1–2 Sv [*Conan and Millot*, 1995]. Moreover, the NC presents variability linked to different scales. Current intensity, dimensions and position change seasonally (the current being narrower, deeper and more intense in winter [*Millot*, 1999]). The NC has a significant mesoscale activity in the form of meanders, eddies and filaments [*Crépon et al.*, 1982; *Sammari et al.*, 1995; *Flexas et al.*, 2002] which has been related to the combination of barotropic processes, due to horizontal shear perturbations, and baroclinic processes, induced by major changes in the stratification [*Flexas et al.*, 2005]. These instabilities can lead to intense meanders, filaments and eddies that develop and propagate along the NC pathway [*Millot*, 1990; *Sammari et al.*, 1995; *Albérola et al.*, 1995; *Flexas et al.*, 2002]. On the continental shelf of the Gulf of Lions the circulation is complex and is linked to the direct and indirect effect of winds [*Millot*, 1990]. In this area, the wind curl together with the complex local orography control the coastal currents, induce upwelling and downwelling processes and favor the formation of eddies on the shelf [*Arnau*, 2000; *Estournel et al.*, 2003; *Millot*, 1990].

[3] On the Catalan continental shelf, the circulation is highly influenced by the NC dynamics (since the shelf is much narrower). In this region, mesoscale variability is frequently associated with the presence of mesoscale anticyclonic eddies over the shelf and slope. The generation of eddies in this area has been associated with different processes. *Tintoré et al.* [1990] observed an anticyclonic eddy off Barcelona which they associated with the spreading of fresh waters from the Gulf of Lions. The authors stated that the eddy could be generated by interaction of the flow with the local bathymetry (namely, the submarine canyon of

[1]Laboratori d'Enginyeria Marítima, Universitat Politècnica de Catalunya, Barcelona, Spain.
[2]Now at AZTI-Tecnalia Marine Research Division, Pasaia, Gipuzkoa, Spain.
[3]LEGI, CNRS, Grenoble, France.
[4]IMEDEA, CSIC, UIB, Palma de Mallorca, Spain.
[5]POC, Toulouse, France.

0148-0227/09/2007JC004245

Figure 1. Schematic of the main characteristics of the ocean circulation and forcing in the study area. Gray arrows indicate the position of the Northern (full line) and Balearic (dashed line) currents. Black arrows show the dominant winds. Asterisks indicate the points of generation of Marseille (ME) and Roussillon (CE) eddies in the model. The bold dot indicates the position of the center of the surveyed eddy ET2001. Bathymetric lines are shown at 200, 1000, 2000, and 3000 m depth.

Palamos). *Font et al.* [1988] proposed the baroclinic instability as the mechanism of formation of meanders and eddies in the vicinity of the Catalan density front. Farther south, *Pascual et al.* [2002] related the generation of an intense warm core eddy to the direct effect of the wind, which induced a warm water tongue of Atlantic Water (AW) to gain negative vorticity.

[4] Antoher hypothesis stated on the origin of Catalan eddies is based on the analysis of series of sea surface temperature (SST) satellite observations [*Arnau*, 2000]. This author suggests that these eddies could be generated in the Gulf of Lions and would then drift southwestward toward the Catalan Sea. The along-slope drifting of anticyclones has been inferred from temperature and velocity time series in the northern part of the Catalan Sea (P. Arnau et al., Combined satellite and field observations of the fate and effects of mesoscale eddies on the Catalan continental shelf (NW Mediterranean), paper presented at the International Symposium ''Satellite-Based Observation: A tool for the study of the Mediterranean basin'', Tunis, 1998), as well as in the southern part [*Jordà*, 2005].

[5] As shown by several authors, these coastal eddies are able to modify the local direction of the circulation and can have a significant impact on the renewal of shelf waters and on the activity of the local ecosystem [*La Violette et al.*, 1990; *Tintoré et al.*, 1990; *Masó and Tintoré*, 1991; *Sabatés and Masó*, 1992; *Durrieu de Madron et al.*, 1999]. Understanding origin and dynamics of these eddies appears essential for the characterization of the hydrological and biological processes occurring in this area.

[6] In 2001 a field experiment in the Catalan Sea permitted to study the 3-D hydrographic properties of an anticyclonic eddy located over the shelf break [*Rubio et al.*, 2005]. The surveyed eddy (hereinafter ET2001) was characterized as having a vertical extent of 100 m, a diameter of 40–45 km, surface velocities of around 0.3–0.4 m s^{-1} and a low-density (high-temperature and low-salinity) core, which suggested that this eddy entrained shelf water. During the survey the eddy drifted southwestward at 6–8 km d^{-1} with an associated volume transport of 0.15–0.3 Sv. In the Catalan Sea, the eddy induced major changes in the density distribution and assisted the subduction of a denser low-salinity water plume. Concerning the genesis of this eddy, the lack of continuity of the SST images due to cloud coverage (which involved gaps of 3–4 days between consecutive images) and the high degree of subjectivity linked to the satellite images interpretation made difficult the discussion of its origin and path. Hypotheses that arose from these observations favored both the local generation over the shelf of the Catalan Sea and the generation in the Gulf of Lions from where this eddy could have been advected toward the Catalan Sea.

[7] In this work we use a numerical model of the NW Mediterranean in order to complement these observations and to carry on the investigation of the origin of eddy ET2001 and, more generally the study of the Catalan Sea anticyclonic eddies. To that end, we analyze the mesoscale structures

Table 1. Main Characteristics of Northwest Mediterranean Model Implementation

Model Main Parameterizations	Value or Approximation of NW Mediterranean Implementation
Horizontal grid scale	3 km × 3km
Number of horizontal nodes	340 × 116
Number of vertical layers	41-z layers
Spatial discretization	c-grid[a]
Temporal discretization	Leapfrog and Asselin filter[b]
External mode time step	5.7 s
Internal mode time step	171.4 s
Advection scheme for temperature and salinity	Mixed[c]
Horizontal viscosity	15 m^2 s^{-1}
Turbulent scheme	Prognostic equation for the EKE[d]
Surface conditions	[e]
Lateral closed boundaries	Free slip conditions[f]
Open boundary conditions	Radiation condition[g] for the external mode and zero gradient for the internal mode. Relaxation layer for the exterior values
Coriolis parameter	β-plane

[a]See *Arakawa and Suarez* [1983].
[b]See *Asselin* [1972].
[c]See *Beckers* [1994].
[d]See *Bougeault and Lacarrére* [1989] and *Gaspar et al.* [1990].
[e]See *Dufau-Julliand et al.* [2004].
[f]See *Estournel et al.* [2003].
[g]See *Oey and Chen* [1992].

present during a six-month period in realistic simulations of the NW Mediterranean and compare their 3-D characteristics to those of the observed eddy. The validation of the model results shows that the model is able to reproduce realistically the main characteristics of the circulation as well as the generation of coherent eddies in two areas of the Gulf of Lions: the coast of Marseille and the southeast coast of Roussillon (both areas are indicated in Figure 1). Therefore, the numerical model allows evaluating the hypotheses of an eddy generation in the Gulf of Lions and its drift toward the Catalan sea. No eddy is locally generated over the Catalan continental shelf where the eddy ET2001 was observed, and the hypothesis of a local origin is consequently not explored in the present work. This paper is organized as follows. Section 2 describes the modeling approach, and in section 3 the results of the model validation are shown. In section 4 we analyses the hypotheses regarding the origin of eddy ET2001 in two areas in the Gulf of Lions and the advection and evolution of these eddies toward the Catalan Sea. Finally, conclusions are presented in section 5.

2. Numerical Modeling

2.1. Model Description

[8] The model used to simulate the circulation in the NW Mediterranean is the 3-D finite differences primitive equations and free surface model Symphonie. A detailed description of this model is given by *Auclair et al.* [2001]. Symphonie assumes as basic hypothesis the noncompressibility, the hydrostaticity and Boussinesq approximation. Spatial discretization is made using a staggered C-grid [*Arakawa and Lamb*, 1977]. The turbulent closure scheme consists on a prognostic equation for the turbulent kinetic energy and on an algebraic formulation of the mixing and dissipation lengths [*Gaspar et al.*, 1990]. The horizontal viscosity coefficient is set to a constant value of 15 m^2 s^{-1}. Model main characteristics are summarized in Table 1.

[9] Surface conditions in the model are imposed through a one-way coupling of the atmospheric variables with the sea surface oceanic model temperature on the basis of an iterative formulation [*Geernaert*, 1990]. The method used in this configuration of the Symphonie has been successfully tested in real cases [*Dufau-Julliand et al.*, 2004].

2.2. Modeling Strategy

[10] The Symphonie model is used in a configuration of the NW Mediterranean to obtain realistic simulations of the circulation during the year 2002. This configuration has been used and validated in a large number of process oriented studies (see for example *Estournel et al.* [2003], *Dufau-Julliand et al.* [2004], or *Petrenko et al.* [2008]). The grid has a horizontal resolution of 3 km (340 × 116 nodes, covering an area of 350,000 km^2) and 41 vertical hybrid $\sigma - z$ layers. The grid is rotated 31° counterclockwise to align the main axis of the domain with the main orientation of the continental slope (Figure 2). The model bathymetry has been generated using the 1′ DBDBV bathymetric database (U.S. Navy Digital Bathymetric Database) bilinearly interpolated in the model grid. Initial and open boundary conditions are obtained from the Mediterranean forecasting system (MFS) general circulation model of the whole Mediterranean Sea [*Pinardi et al.*, 2003] at 1/8° of resolution. The open boundary conditions scheme consists of a set of radiative

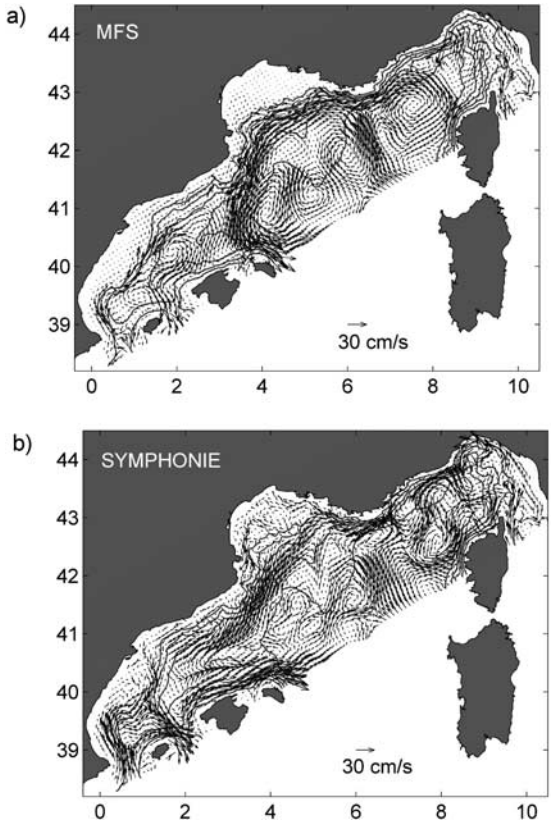

Figure 2. Model domain. (a) MFS general model (providing initial conditions and open boundary forcings) and (b) Symphonie model velocity fields at 50 m depth in June 2002.

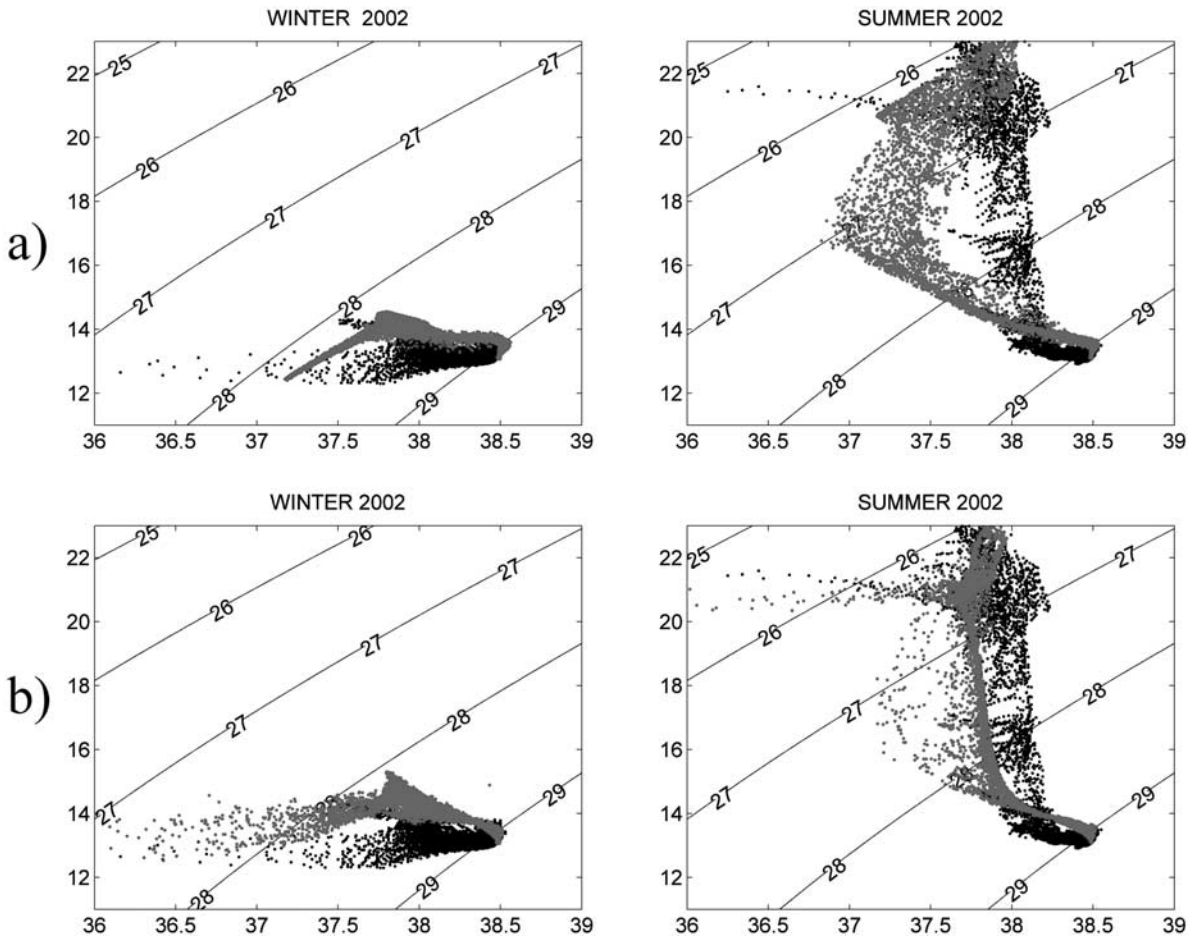

Figure 3. Three-month average TS diagrams from model (gray dots) and climatologies (black dots) in winter and summer 2002 from (a) MFS general circulation model and (b) Symphonie model.

equations, described by *Marsaleix et al.* [2006], combined to a nudging boundary layer. Inside this boundary layer the model variables are relaxed toward their external counterpart value in order to avoid drifts between modeled and forcing fields. The relaxation is done through a restoring term in the model equations of the prognostic variables. The restoring timescale τ_r is such that this additional term progressively vanishes with the distance to the open boundaries. The nudging layer width has been set to 15 grid points (45 km). The relaxation timescale for the external mode (barotropic velocities) is set to 0.05 days. For the internal mode variables (3-D velocities, temperature and salinity) it is set to 1 day. The boundary values are updated daily.

[11] Atmospheric variables which define the surface forcing are obtained from regional analyses performed with the atmospheric model ALADIN (Météo-France). ALADIN is a data assimilating model that has been successfully used in the same region to provide the surface forcing of ocean circulation models in process-oriented studies [*Estournel et al.*, 2003; *Dufau-Julliand et al.*, 2004] and in operational systems (MFS project [*Pinardi et al.*, 2003]). Atmospheric data (short wave radiation, cloudiness, 10 m winds, potential temperature and humidity) are provided every 3 h with a horizontal resolution of 10 km. Daily runoff values for the main rivers (Rhône, Petit Rhône, Hérault, Aude, Orb and Ebro) are provided by the "Compagnie du Rhône", the "Direction Régionale de l'Environnement of the Langedoc Roussillon", and the "Confederación Hidrográfica del Ebro".

[12] The model is run for the whole year 2002. Our investigation focuses on the period from March to September 2002 and uses the model daily outputs. MFS simulations in the NW Mediterranean for the year 2002 are used to provide initial conditions and open boundary forcing for the period (it was the longest available set of high-resolution simulations driven by high-resolution realistic forcing available at this time). It is worth emphasizing that our objective was to obtain a comprehensive analysis of the mesoscale phenomena and not to reproduce a particular observed event.

3. Validation of the Modeling

3.1. Hydrology

[13] Although the ability of this model configuration to realistically simulate the large-scale and mesoscale features of the ocean circulation of the NW Mediterranean has been demonstrated in several studies [*Estournel et al.*, 2003; *Dufau-Julliand et al.*, 2004; *Petrenko et al.*, 2005; *Gatti et al.*, 2006; *Petrenko et al.*, 2008; *Ulses et al.*, 2008] we present here a short validation of the simulation we carried out on year 2002.

[14] In Figure 3 we compare model TS diagrams with those obtained from climatological data (we use MEDAR

(http://modb.oce.ulg.ac.be/medar/welcome.html) and MODB (http://modb.oce.ulg.ac.be/modb/welcome.html)) (Mediterranean databases). Summer and winter three-month average TS diagrams have been calculated for the regional Symphonie model and the MFS model for an area which encloses the shelf and slope of the Catalan Sea and the Gulf of Lions. The same geographic area and periods have been used to extract summer and winter TS climatologic data. Both numerical models show systematic errors in their representation of the TS properties. Model waters are globally too warm in winter, and too fresh at intermediate depth and too warm at the bottom in summer. In the case of the MFS general circulation model, differences in terms of salinity are significantly greater in summer (Figure 3), especially for waters of intermediate depth in the density range of $28 < \sigma_0 < 26.5$. Note that the freshest shelf waters present in the climatology in winter (the 13°C waters the salinity of which varies between 36 and 37 practical salinity units (psu)) and in summer (the 21°C waters with salinity less than 37.5 psu) are not represented in MFS, likely due a poor representation of river runoff. The TS misfits between the MFS general circulation model and climatology are transmitted to the regional model through the initial and open boundary conditions. However, the internal dynamics of the higher-resolution model allows to partially correct those misfits. First, the representation of the low-salinity shelf waters is greatly improved, since these waters are now present with properties comparable to climatology. Second, the salinity misfit seen in summer for the waters at intermediate depth ($28 < \sigma_0 < 26.5$) is considerably reduced, and the shape of the TS profile is now comparable to climatology. In the winter period, the quality of the regional and general circulation models is similar with both model predicting higher temperatures than climatology. A careful look at the regional model results in the deep layers showed that these layers are little modified in a 1-year period (see the small seasonal changes in water masses between 28.5 and 29 isopycnals in Figure 3). Therefore, even if the regional model is able to better represent the dynamics of the region, the simulation is not long enough to correct initial misfits in the deep layers. On the other hand, the upper layers are much more variable. Surface heat fluxes, wind and river runoffs modify their characteristics in shorter timescales (from days to weeks). Consequently, a better representation of the dynamics in the regional model leads to an improvement of the water mass characteristics in those layers, correcting the initial misfits.

[15] In terms of mean values, Symphonie simulations present waters around +0.4°C warmer and −0.3 psu fresher than climatology at shallow and intermediate levels. As the regional model significantly improved the representation of the vertical gradients we can expect the disagreements in terms of absolute values not to have a major impact on the quality of the simulations. Moreover, the comparison of the model surface temperature and salinity model surface fields with satellite imagery (as revealed in Figures 4 and 6) shows that the model reproduces realistically the horizontal gradients and surface structures (i.e., the Rhône plume dynamics, the surface cooling of shelf waters, the development of upwelling during strong NW wind events). A comparison between simulations and AVHRR SST fields is shown in Figure 4 during a NW wind event in the Gulf of Lions which is responsible for the growth of several areas of upwelling along the coast, as described by *Millot* [1990]. This upwelling event is induced by NW winds blowing from 5 August to 13 August over the Gulf, with maximum velocities of 15 m s^{-1}. Model SST fields are compared to contemporary satellite SST data (AVRHH/NOAA from the Spanish SAIDIN database: http://ers.cmima.csic.es/saidin/sst.html). Because the model is not constrained by data assimilation and the model resolves the mesoscale turbulence, the comparison with observations remains qualitative and is done regarding the large-scale patterns and the signature of the mesoscale and coastal processes. On 5 August (Figures 4a and 4d), before the wind event starts, the gulf surface waters present cold temperature at shallow depths while a warm water tongue evidences the entrance of the NC at the northeast of the gulf. After the wind event starts, on 7 August, model and satellite SST show the first cells of coastal upwelling along the coast of Marseille while the temperatures start cooling in the rest of the Gulf (Figures 4b and 4e). In the simulations the cooling of surface waters is less marked although the apparition of upwelling cells off Marseille is correctly reproduced. Finally, one week after the beginning of the wind event (Figures 4c and 4f) model and SST satellite data present similar global situations. While the continental shelf of the gulf is occupied by cold waters the signal of warm waters linked to the entrance of the NC into the gulf disappears west of the Hyeres Islands. The comparison also shows similar temperature gradients at the mesoscale, which suggests the existence of a realistic eddy field. Globally, the model correctly reproduces the cooling of surface waters and the upwelling processes with similar timescales and space scales that the observed ones, although surface temperatures are in general higher in the simulations.

3.2. Currents

[16] Characteristics of the Northern Current in the regional Symphonie model are examined. The path of the current (Figure 2a) along the slope of the NW Mediterranean shelf is correctly reproduced in most parts of the domain (i.e., Ligurian Sea, Gulf of Lions and northern part of the Catalan Sea). This is for a part due to the open boundary conditions imposed by the MFS general circulation model at the northeast side of the modeled domain (see Figure 2b), and more specifically to the representation of the incoming East and West Corsica currents which have adequate 3-D structure and intensities (not shown). However, the conditions imposed by the MFS model at the southwest side of the open boundary are far less satisfactory. In this later model (Figure 2b) the NC separates from the slope at the entrance of the Catalan Sea, flowing offshore along the northern side of Balearic Islands shelf, instead of flowing southwest along the Catalan slope. This circulation scheme strongly disagrees with field observations that show a NC flowing southwestward along the slope until crossing the Ibiza channel [*Font et al.*, 1995; *Millot*, 1987; *Pinot et al.*, 2002]. The regional model, with its higher resolution and a better representation of the bottom topography, is able to correct this flaw after a few months spin-up. The circulation in August 2002 (Figure 2a), for example, shows a NC which is correctly placed over the slope south of the Palams canyon. Although the picture is not perfect yet, it represents a clear improvement of the current path. For the analyzed period,

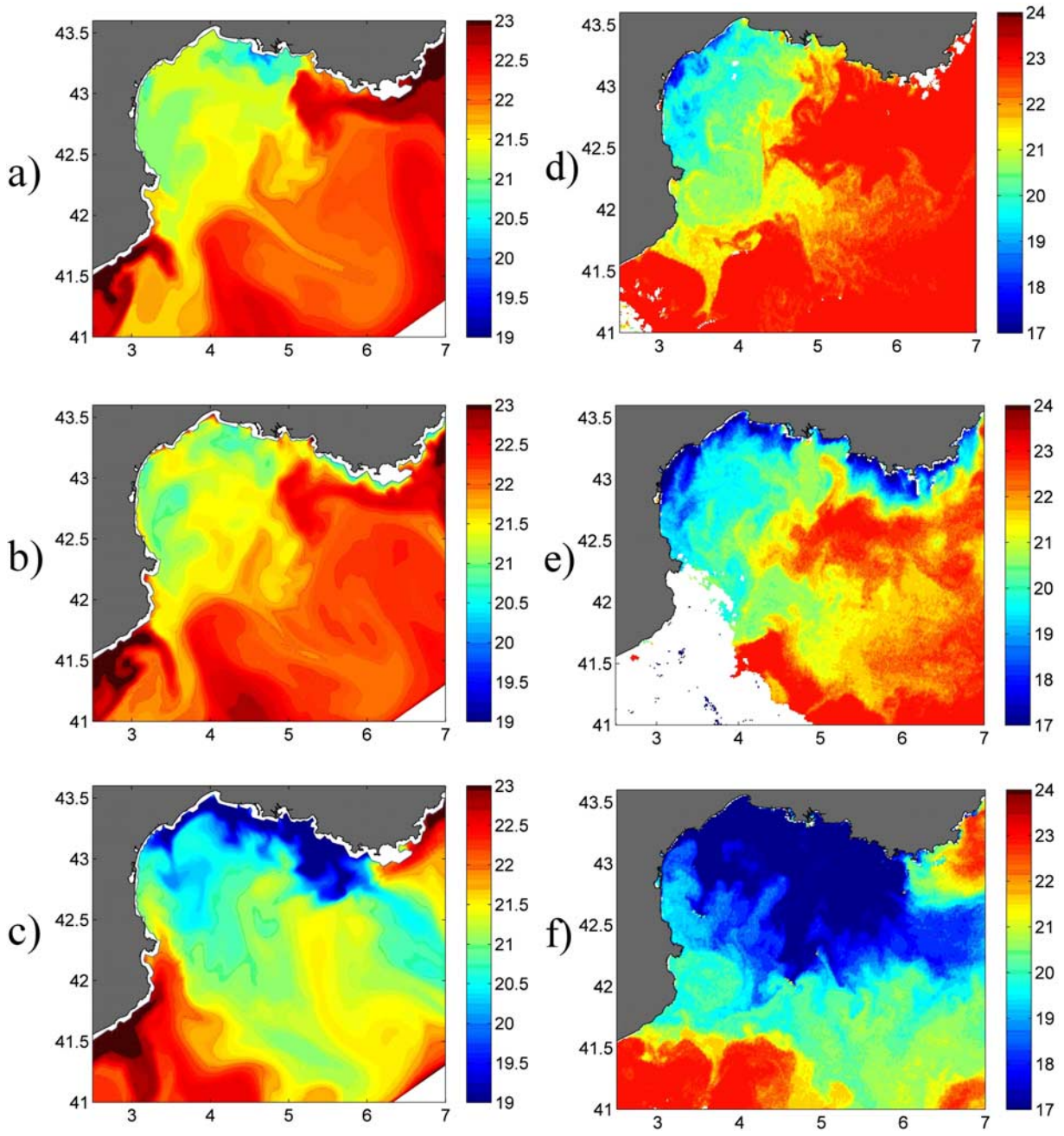

Figure 4. (a, b, c) Model and (d, e, f) satellite surface temperatures during a NW wind event in the Gulf of Lions. The evolution of the coastal upwelling on the shelf of the NW and NE Gulf of Lions is shown for 5 (Figures 4a and 4d), 7 (Figures 4b and 4e), and 14 (Figures 4c and 4f) August 2002.

the Symphonie model NC flows most of the time along the slope in the northern part of the Catalan Sea (Figure 2b). Since we focus on eddy generation processes occurring in the Gulf of Lions and the northern border of the Catalan Sea (north of Palamos canyon) we consider that flaws remaining in the representation of the Northern Current farther south (i.e., downstream) should not have significant impact on our results concerning eddy structure and dynamics.

[17] The NC in the Symphonie model has a vertical structure and volume transport (maximum values over 2 Sv and mean values of 1.2 Sv) which are in agreement with observations [*Albérola et al.*, 1995; *Conan and Millot*, 1995]. *Conan and Millot* [1995] observed (from February to July 1992, off Marseille) a NC 400–500 m deep with velocities between 0.3 and 0.5 m s^{-1} and transports between 0.5 and 1.75 Sv. The seasonal variability of the model NC (not shown), i.e., its changing location over the slope, its changes in 3-D structure and intensity are also reproduced in accordance what is described by previous works [*Albérola et al.*, 1995; *Conan and Millot*, 1995; *Sammari et al.*, 1995]. In winter model NC is located between the 1000–2000 m isobaths, has a vertical extent of about 400 m, is about 30 km wide and is characterized by surface velocities of about 0.4 m s^{-1}. In summer the model NC is shallower

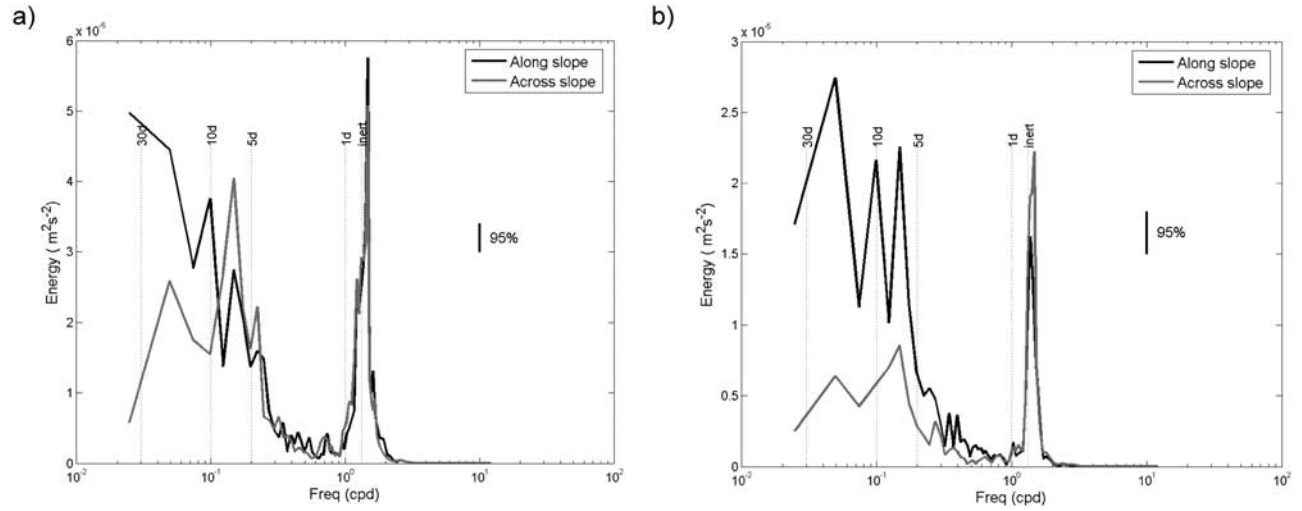

Figure 5. Frequency analysis of the along-slope (black) and cross-slope (gray) components of the NC velocity in front of Marseille (43°N, 5.23°E) at (a) 100 and (b) 300 m.

(200 m), narrower (20 km) and weaker (surface velocities around 0.2–0.25 m s^{-1}). The frequency analysis of the along-slope and across-slope components of the model NC velocity at the NE of the Gulf of Lions (43°N, 5.23°E) shows that the variability at smaller scales is realistic (Figure 5).

[18] Energetic oscillations are seen in the inertial band (~17.7 h) at 100 m and 300 m, as observed by *Flexas et al.* [2002] in this area. Moreover we identify two maxima in the mesoscale band, at 3.5 and 7 days, in the across-slope component which are in accordance with previous in situ measurements. Observations indicate that these two maxima can be related to the NC meandering [*Flexas et al.*, 2002; *Sammari et al.*, 1995; *Durrieu de Madron et al.*, 1999]. In the model, high energy levels associated with the band over 10 days are observed in the along-slope and across-slope directions. These oscillations can be related to current intensity variations [*Sammari et al.*, 1995] and high-amplitude meanders [*Albérola et al.*, 1995], respectively.

[19] Finally, the capability of the model of reproducing the circulation over the shelf in response to different wind patterns has been demonstrated by *Estournel et al.* [2003]. In the simulations for the year 2002, the wind-induced coastal currents and the generation and evolution of upwelling and downwelling phenomena over the shelf are in accordance with observations (see Figure 4).

3.3. Mesoscale Anticyclonic Eddies

[20] During the simulation, several mesoscale eddies are observed to develop and drift over the shelf and along the slope, most of them being anticyclones. Cyclonic eddies are also present but they are smaller and have short lifetime. Although most model eddies loose their coherency a few days after they are generated, we observe 9 anticyclonic eddies with lifetimes going from one to several weeks (Table 2). In the simulations, these long-lived eddies are advected by the currents covering distances over 100 km and following complex paths. We observe eddy-eddy interactions (merging) and eddies interacting with the bathymetry and the slope current: as a result of these interactions eddies become more intense or weaken and present major changes in their drift velocities. Typically their diameters are around 30–40 km, which is in agreement with previous observations [*Rubio et al.*, 2005; *Flexas et al.*, 2002; *Arnau*, 2000].

[21] The generation of long-lived coherent eddies is observed in two areas in the Gulf of Lions: over the continental slope off Marseille and over the continental shelf off the southeast Roussillon coast (Figure 1). No eddies are

Table 2. Main Characteristics of Marseille and Roussillon Eddies[a]

	Generation Point								
	Longitude (°E)	Latitude (°N)	Lifetime (days)	θ Maximum (km)	Depth (m)	$V_{50\ m}$ (m s^{-1})	$T_{50\ m}$ (°C)	$S_{50\ m}$ (psu)	Vdrift (km d^{-1})
EM0325	6	43	8	22	400	0.2	+0.1	+0.5	6.75
EM0331	6.01	42.9	17	28	400–500	0.3	+0.1	+0.5	9
EM0406	6	42.9	11	20	400	0.2	+0.1	+0.5	8
EM0510	6.01	42.9	16	28	300–400	0.2	+0.5	+0.5	7
EM0619	5.97	42.9	20	35	300	0.2	+1	+0.5	7.5
EC0413	3.38	42.2	18	25	80–100	0.2	−0.2	−0.25	6.5
EC0520	3.35	43.2	47	25	200–400	0.25	+0.5	−0.1	6.8
EC0627	3.4	42.2	10	16	60–70	0.15	+1.5	−0.2	7.1
EC0715	3.38	42.2	52	35–40	80–100	0.35	+1.5	−0.15	5.7

[a]Characteristics of Marseille eddies identified as "EMmmdd", where "mmdd" stands for month ("mm") and day ("dd") of generation and Roussillon eddies identified as "ECmmdd", where "mmdd" stands for month ("mm") and day ("dd") of generation. Values shown are generation point, lifetimes, maximum diameter reached during their lifetime, mean vertical extent, eddy mean surface velocities, temperature and salinity anomalies (between eddy core and surrounding waters), and eddy drift velocities.

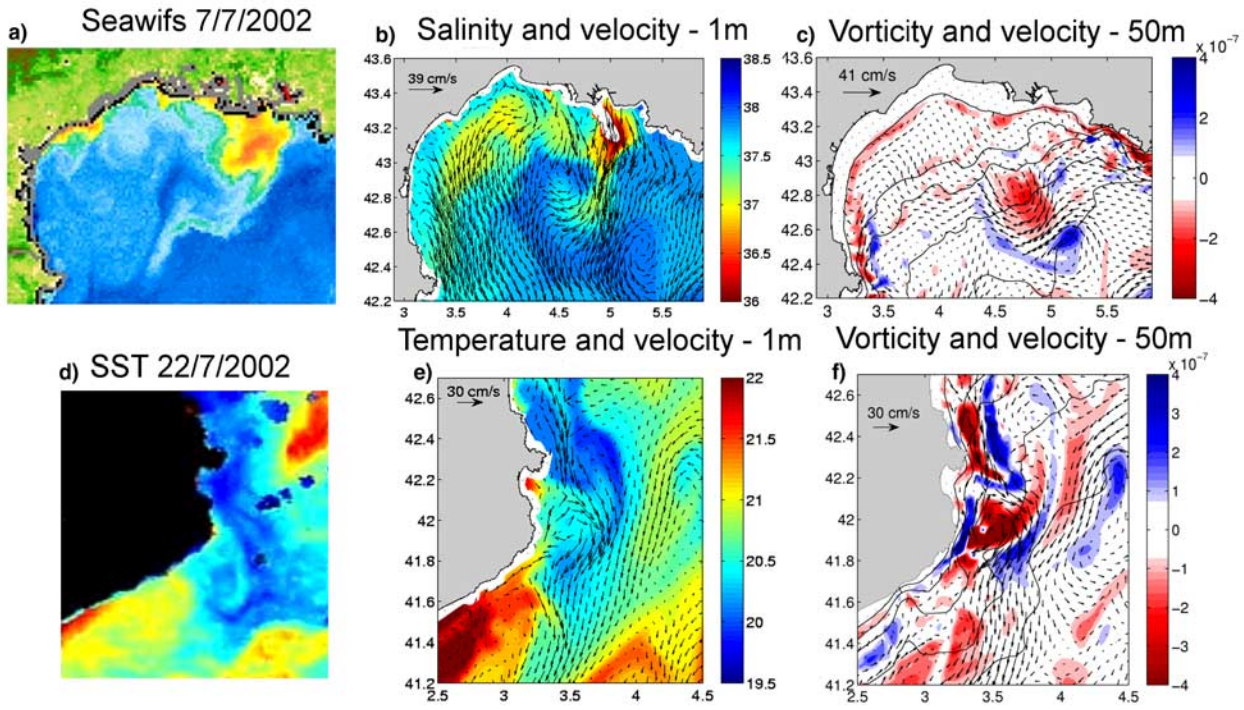

Figure 6. (a) Satellite Sea-viewing Wide Field-of-view Sensor (SeaWiFS) images where we can observe an anticyclonic eddy over the slope of the Gulf of Lions and model snapshots at the corresponding date of (b) salinity and velocity fields at 1 m (center) and (c) velocity and vorticity fields at 50 m. (d) Satellite SST image where we can observe an anticyclonic eddy at the south of Creus Cape and model snapshots at the corresponding date of (e) temperature and velocity fields at 1 m and (f) velocity and vorticity fields at 50 m.

observed to generate locally over the Catalan shelf where ET2001 was detected by in situ measurements. During the simulation, 5 eddies generate at the coast of Marseille and 7 at the southeast of Roussillon. Figure 6 shows an example of these eddies and their comparison through contemporary satellite imagery to their real counterparts. Although there are slight differences concerning their positions, model eddies present realistic horizontal dimensions and TS gradients.

[22] In the Catalan Sea we observed 4 anticyclonic eddies that drifted southwestward contouring the continental shelf during the six-month period of simulations analyzed. Catalan model eddies have hydrodynamic characteristics very similar to those of eddy ET2001. Figure 7 shows the comparison in terms of horizontal velocities and TS structure between the observed eddy ET2001 (Figure 7a) and EC0715 (Figure 7b) model eddy in the Catalan sea. As we can see, these two eddies, generated during similar stratification conditions and located between the 200 and 1000 m isobaths, show comparable dimensions with diameters around 40 km and 80–100 m of vertical extent. Observed and model horizontal velocity fields at 60 m reveal mean velocities of 0.3–0.4 m s^{-1}. Concerning the hydrographic structure, Figure 7 shows the vertical TS profile (surface to 120 m) extracted at the center of each eddy, the center being defined as the point of maximum relative vorticity at 50 m. The section of the profile comprised between 30 and 90 m depth is indicated in Figure 7 in order to facilitate the comparison. Although the core of the model eddy is slightly less dense and less homogeneous in terms of salinity (because of the differences in the stratification conditions between July and September and also to the bias in the model TS commented in section 2) both eddies present similar structures, being characterized by low-density (high-temperature and low-salinity) cores.

4. Hypotheses on the Generation of the Catalan Eddy

[23] We investigate two hypotheses concerning the origin and path of the Catalan Sea eddies. The first one formulates that the eddies generate off Marseille and in the second one, the eddies are generated at the southeast coast of Roussillon. In both cases, after being generated Marseille and Roussillon eddies would be advected by the local circulation toward the Catalan Sea. We investigate the generation mechanism, characteristics and evolution of these two groups of eddies and we compare them to the eddy ET2001 observed in the Catalan Sea in 2001.

4.1. Marseille Eddies

4.1.1. Eddy Generation

[24] 5 anticyclones develop in this area between 25 March and 19 June. Three of them have a lifetime longer than two weeks (Table 2). Eddy generation occurs always around 6°E, 43°N (Figure 1), over the slope (i.e., over the 600–1000 m isobaths). In this point the NC, which leaves the Ligurian Sea to follow the slope of the Gulf of Lions, finds a major change in the orientation of the coast and slope.

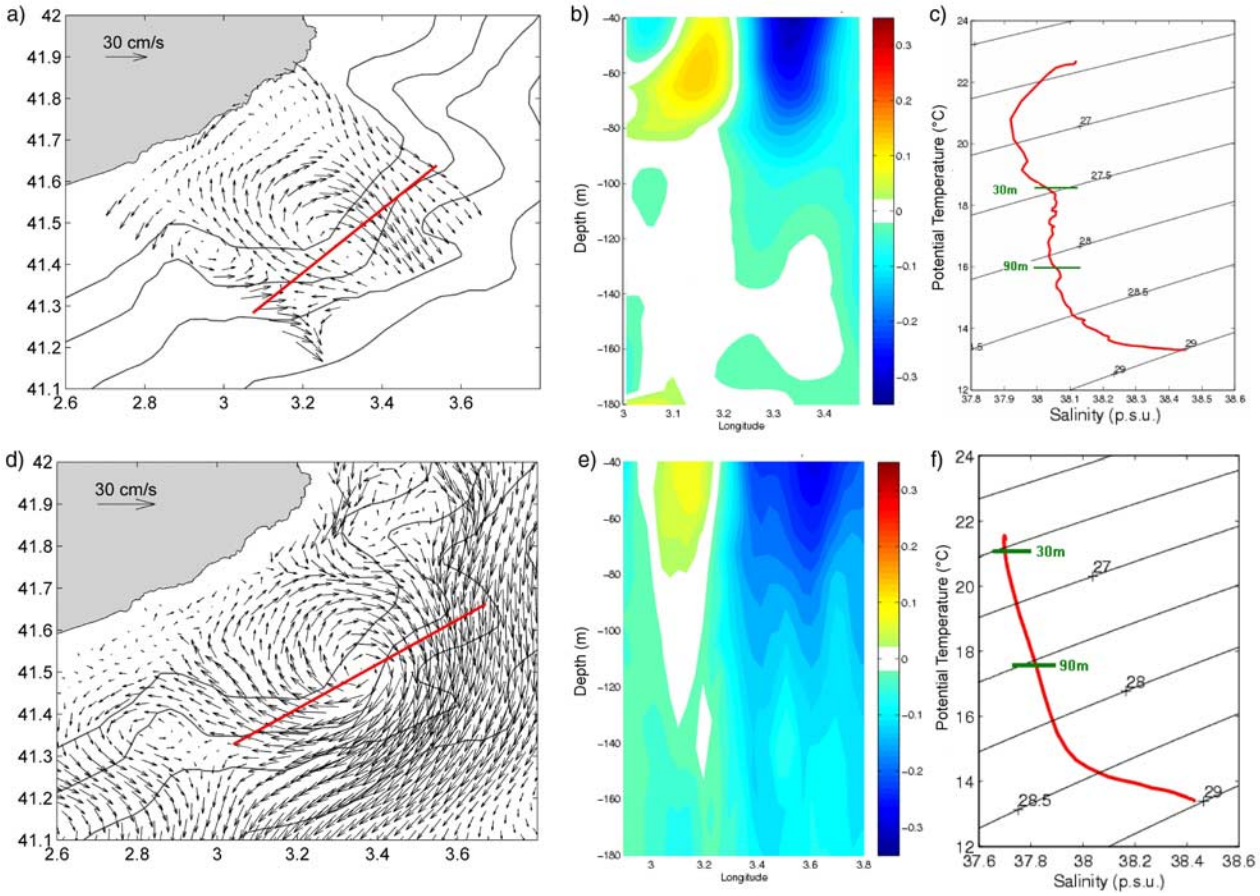

Figure 7. Main characteristics of (a, b, c) eddy ET2001 observed in the Catalan Sea in September 2001 and (d, e, f) EC0715 model eddy (model results for 31 July 2002). Velocity field at 60 m (Figures 7a and 7d), vertical section of the N-S velocity component (the section is marked by a red line in Figures 7a and 7d) (Figures 7b and 7e), and TS diagram at the center of each eddy (Figures 7c and 7f).

This change is especially significant in front of the coast of Toulon since at the east of this city the shelf widens locally because of the presence of Hyères Islands.

[25] Figure 8 shows the generation of one of Marseille eddies on 19 June. This eddy, called eddy EM0619 is generated around 5.9°E 42.9°N and presents a diameter around 10 km. At the time the eddy is generated, the NC has velocities around 0.4 m s^{-1} at 50 m and low-density warm waters (σ_t = 28.05, T $\sim$ 15.6°) are present near the coast associated with the NC path. On 19 June, eddy EM0619 has velocities of 0.1–0.15 m s^{-1} and a vertical extent of 250 m. During the following days, eddy EM0619 grows (diameter around 26 km on 25 June), becoming more intense (0.2 m s^{-1} on 25 June) and deeper (around 400 m on 25 June). During its generation and growth, the eddy incorporates coastal low-density waters to its core. As eddy EM0619 develops, the NC which contours the eddy tends to flow more offshore. On 25 June eddy EM0619 starts to drift to the SW advected by the NC, reaching the maximum diameter (35 km) one week later.

[26] To evaluate the effect of the main local forcings on eddy generation we have carried out a number of sensitivity experiences in which we have suppressed alternately the wind forcing and the Rhône river runoff. These experiences have been performed during different periods between February and August (not shown). In the case of null runoff river simulations results reveal that buoyancy inputs from river runoff have no direct effect on eddy generation. In all cases, eddies generate and present the same intensity and structure, being only observed some differences in terms of temperature and salinity surface distributions. In the case of simulations where the wind forcing is suppressed, eddy generation and growth is not affected in the short term revealing that wind forcing does not play major role. However, in the long term (i.e., after two to three months of simulations) the suppression of the wind forcing affects globally to the intensity of the circulation. Namely, the intensity of the NC tends to weaken and when this happens, eddy shedding does not longer take place. This result suggests that the generation of eddies is related to the intensity (and shear) of the NC.

[27] The examination of model fields during the different episodes of eddy generation (as the one showed in Figure 8), suggest that in this area eddy generation is linked to a flow separation mechanism with takes place during NC intensifications. During the intensifications and because of the local variation of the slope orientation the NC tends to separate from the slope inducing eddy shedding downstream Hyères

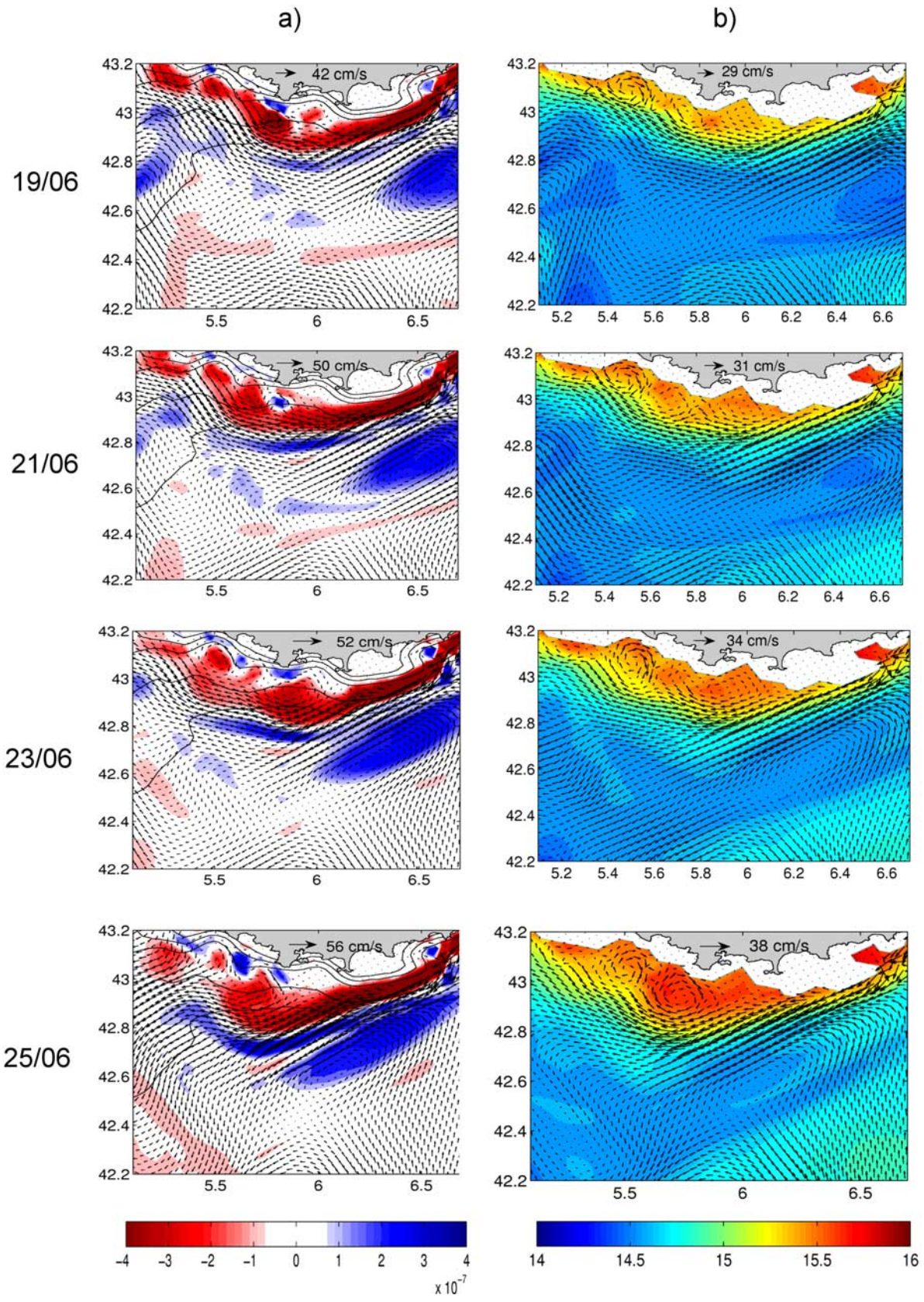

Figure 8. EM0619 Marseille eddy generation. Shown are five successive snapshots of (a) relative vorticity and velocity fields at 10 m and (b) temperature and velocity fields at 100 m.

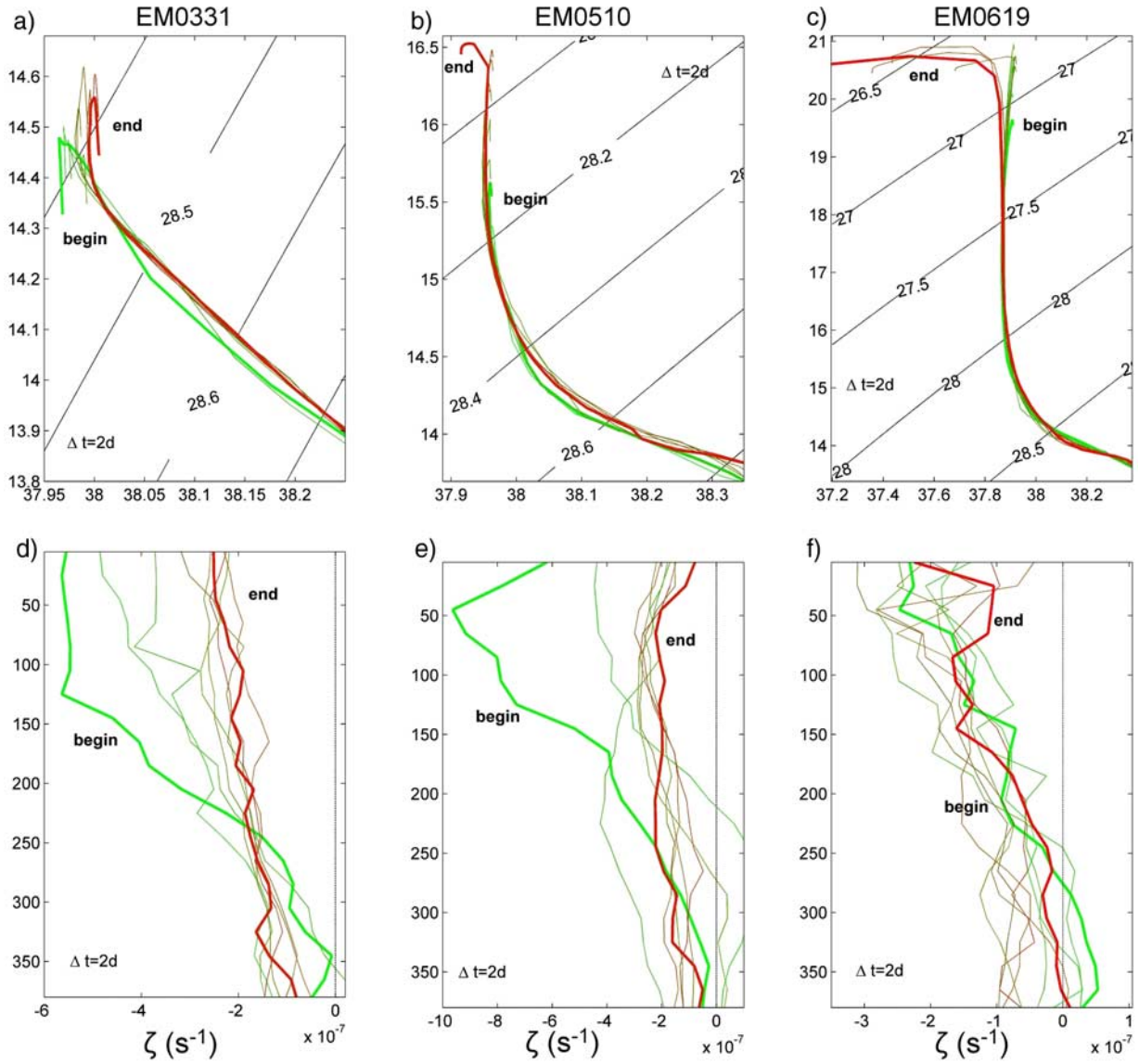

Figure 9. Time evolution of (a, b, c) TS and (d, e, f) relative vorticity profiles of Marseille eddies EM0331 (Figures 9a and 9d), EM0510 (Figures 9b and 9e), and EM0619 (Figures 9c and 9f). Green profiles correspond to the beginning of eddy lives, and red profiles correspond to the end of eddy lives. Lines show the time evolution of the profile at a 2-day interval.

Islands. In the simulations, NC separation and eddy shedding take place when current intensities are over 0.3 m s^{-1}.

4.1.2. Eddy Dynamics and Path

[28] As we can see in Table 2, Marseille eddies are characterized by maximum diameters of 30 km. The vertical extent of these eddies is linked to the vertical extent of the NC, reaching between 300 m (eddy EM0619, generated in June) and 500 m (eddy EM0331, generated in March). Maximum velocities are observed in the first 100 m associated with the maximum velocities of the slope current. These eddies are characterized by a low-density core as they incorporate the NC warmer and more saline waters which are in contrast with the cold and continentally influenced Gulf of Lions waters.

[29] In Figure 9 we show the evolution of the vertical TS and relative vorticity profiles for the three longest-lived eddies. We plot these profiles from 10 to 400 m at the maximum of relative negative vorticity within the center of each eddy, determined from the relative vorticity and velocity daily fields at 50 m. The most important variations in the TS distribution are observed in the first 50 m. From the beginning to the end of their lifetime, temperatures of EM0510 and EM0619 cores at 50 m increase by 1°C. In the case of eddy EM0331 the increase is only 0.2°C as temperatures in the Gulf of Lions are more homogeneous at the time this eddy develops (late Mars). Salinities present smaller variations which are only significant in the case of EM0619 as it incorporates shallow continental waters (37.2–37.6 psu) during the second part of its lifetime. Concerning the relative vorticity profiles (Figures 9d, 9e, and 9f), we can observe that eddy vertical profiles tend to be more homogeneous with time as the attenuation of the

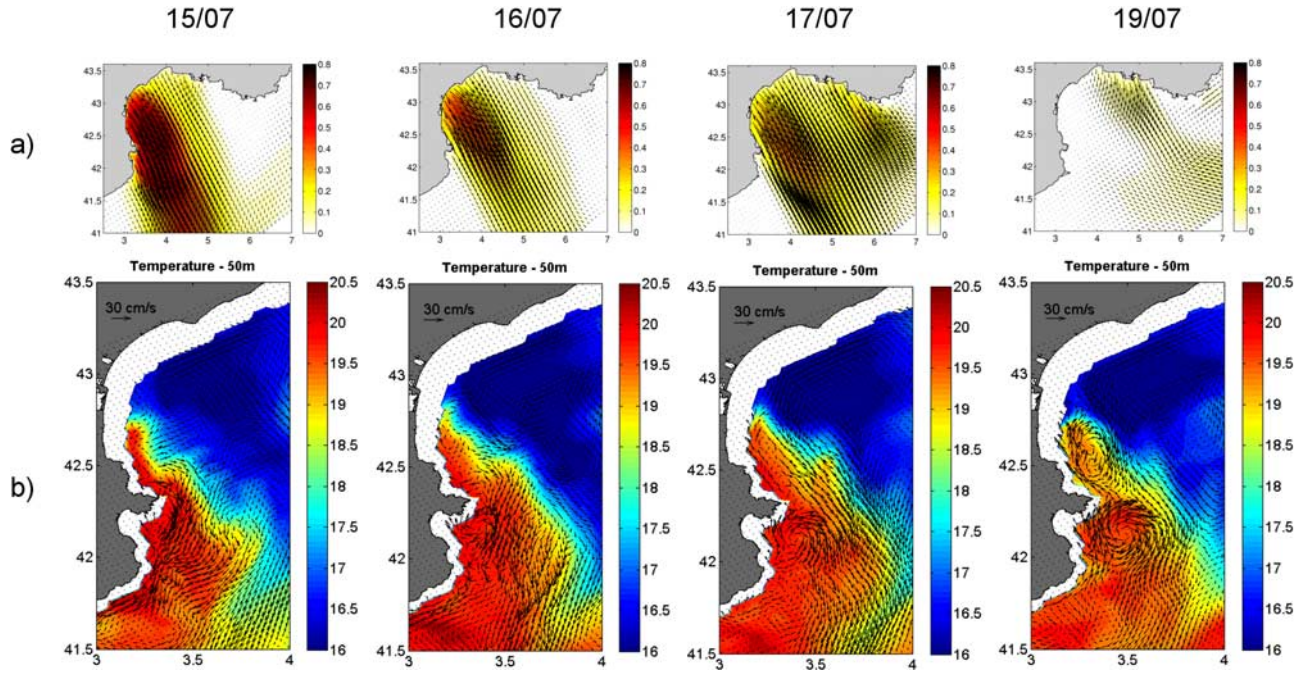

Figure 10. Genesis of EC0715 Roussillon eddy. Snapshots of (a) the wind field and (b) the temperature and velocity field at 50 m at four different times.

velocities (and diameters) is more accentuated in the shallower levels. Their vertical extension remains constant until the end of their lifetime.

[30] Concerning their trajectories, these eddies are advected southwestward by the NC following the slope at 7–9 km d^{-1}. Model eddies drifting velocities are in accordance with SST satellite observations in this zone [*Arnau*, 2000]. During their southwestward drift, model eddies weaken until they fade in the Gulf of Lions, 10 and 20 days after they are generated, and no Marseille eddies has been seen to reach the Catalan Sea in the model simulations. This result differs from the analysis of satellite imagery of SST by *Arnau* [2000] which suggests that this drifting may occur repeatedly during the year. The short lifetime of the model Marseille eddies (which prevents them to reach the Catalan Sea) is not a numerical artefact. Indeed, the numerical dissipation used in the model (a Laplacian viscosity operator with a coefficient $v = 15\ m^2\ s^{-1}$) cannot explain for this short lifetime (a 70-day e-folding timescale can reasonably be associated with this value of v much longer than the 10- to 20-day eddy lifetime [see *Holland*, 1978]). A sensitivity experiment has been carried out that verifies the low sensitivity of the eddy lifetime to numerical dissipation. The model was rerun from 20 June to 20 September (the period coinciding with the generation and development of eddy EM0619) with a value of $v = 3\ m^2\ s^{-1}$ (corresponding to a 350-day e-folding timescale). The eddy lifetime was barely increased by 2 to 3 days. Therefore, the short lifetime of the model Marseille eddies should be considered as a dynamical property resulting from their interactions with the environment (topography, slope current, other eddies). The apparent contradiction between the model results and the analysis of *Arnau* [2000] on the possibility of the Marseille eddies to enter the Catalan Sea thus remains and will require additional investigation. Note however the consistency of the model results: model Marseille eddies have a vertical extent which is much deeper, and core TS properties that are quite different, than those of the observed eddy in the Catalan sea, evidencing that these two types of eddies do not have the same origin.

4.2. Roussillon Eddies

4.2.1. Generation Mechanism

[31] 7 anticyclonic eddies are generated in this area from April to August 2002. Four of these eddies have lifetimes over one week, we show their main characteristics in Table 2. Eddy generation occurs downstream the Creus Cape around 42°N, 3°E over the shelf (between the 100–150 m isobaths) linked to strong NW wind events in the Gulf of Lions. In Figure 10 we show the generation of one of the Roussillon eddies at the middle of July 2002 (eddy EC0715) during a strong NW wind event. Wind event starts on 14 July (not shown) affecting the SW part of the Gulf of Lions with maximum velocities of 19 m s^{-1}. Maximum wind intensities occur on 15 July with velocities of 21 m s^{-1}. On 15 July there is a strong stratification, the seasonal thermocline being located around 30–50 m. A weak coastal current (0.26 m s^{-1} at 50 m) follows the southwest coast of the Gulf of Lions and surface currents are oriented to the SW with velocities around 0.3 m s^{-1} at 50 m. As a consequence of the southwestward transport of surface waters, a downwelling begins to develop along Roussillon coast. The following days, in response to the NW wind event, surface circulation is intensified along the coast. On 16 July, the coastal current presents maximum velocities around 0.6 m s^{-1} and reaches 60 m depth. A countercurrent, with maximum velocities of 0.3 m s^{-1} at 50 m appears downstream Creus Cape. On 17 July wind intensity decays and as we can observe in Figure 10b the circulation is driven by the density field. The coastal current extends from surface to 80 m with velocities around 0.35 m s^{-1}. Thus, after the wind event, the interaction

of this density-driven current with the cape accounts for the growth of the eddy. On 17 July eddy velocities at 50 m are around 0.4 m s^{-1} and the eddy has a vertical extension of 80 m. From 17 July to 19 July eddy EC0715 grows significantly coinciding with the weakening of the downwelling (note that in these dates both, the wind and the coastal current, are weak). On 19 July, the depth of eddy EC0715 reaches 100 m and it is characterized by surface velocities around 0.5 m s^{-1} and a diameter of 36 km. It is located between the 100 and 200 m isobaths and its core contains the warmer downwelled waters. After that, the eddy starts to drift toward the slope and then is advected by the NC toward the Catalan Sea.

[32] As in the paper by *Böning and Budich* [1992] we examine the transfers of kinetic energy (KE) and available potential energy (APE) between the mean field and the eddy field to investigate the processes accounting for eddy generation in this area. We define:

$$MKE \Rightarrow EKE = -\int \overline{u'u'}\frac{\partial \overline{u}}{\partial x} + \overline{v'v'}\frac{\partial \overline{v}}{\partial y} + \overline{u'v'}\left(\frac{\partial \overline{v}}{\partial x} + \frac{\partial \overline{u}}{\partial y}\right)dz$$

$$MAPE \Rightarrow EAPE = \frac{g}{\rho_0}\int \left(\frac{\partial \overline{\sigma}}{\partial z}\right)^{-1}\left(\overline{u'\rho'}\frac{\partial \overline{\rho}}{\partial x} + \overline{v'\rho'}\frac{\partial \overline{\rho}}{\partial y}\right)dz$$

where overbars indicate temporal average and primes represent turbulent quantities, ρ_0 is a reference density, $\overline{\sigma}$ is the mean density computed at each horizontal level, MKE is mean kinetic energy, EKE is eddy kinetic energy, MAPE is mean available potential energy, and EAPE is eddy available potential energy. When these quantities are positive they indicate transfers from the mean to the eddy field, MKE $\Rightarrow$ EKE being transfers related to barotrophic processes and MAPE $\Rightarrow$ EAPE transfers related to baroclinic processes. Time averages are calculated for the six months of simulations, from February to August. Deviations are calculated as the difference of the daily fields to this average. We have calculated the six-month average of the vertically integrated transfers from 10 to 400 m (not shown). Energy transfers suggest that in this area both barotrophic and baroclinic processes are present off Roussillon coast. MKE $\Rightarrow$ EKE transfers occur in the coastal current and are maximum around Creus Cape (associated with the strong horizontal shear near the cape). MAPE $\Rightarrow$ EAPE transfers occur off Roussillon coast over the shelf, in the area affected by downwelling processes. To better understand the generation mechanism of these eddies we have examined the energy transfers during a typical eddy generation event. In Figure 11 we show the 3-day average of EKE and APE transfers during two periods within the generation of eddy EC0715: from 13 July to 16 July (during the wind event) and from 17 July to 20 July (after the wind event). MKE $\Rightarrow$ EKE transfers occur during both periods associated with the interaction of the coastal current (first the wind-induced current and then the density-driven current) with the bathymetry. After the wind stops, MAPE $\Rightarrow$ EAPE transfers become significant indicating that, although during the wind event eddy generation is mainly barotropic, baroclinic processes may also account for the growth of the eddy when the wind forcing weakens. This baroclinic contribution is associated with the release of available potential energy during the relaxation of the downwelling.

[33] Sensitivity tests confirm the major role of the wind forcing at Roussillon since in the no wind simulations no eddy is generated (not shown). Concerning buoyancy inputs, in the no river simulations eddy generation is not affected in the short term. However, after four to five months without river inputs shelf waters become significantly less buoyant and as a consequence the downwelling can reach deeper levels. In the simulations without river runoff temperature signals associated with the downwelling and eddies are more intense (not shown).

[34] The joint analysis of model fields, energy diagnostics and sensitivity tests, shows that in this area eddy generation is triggered by NW winds events in the Gulf of Lions through the intensification of the coastal circulation. In the simulations, the coastal current is observed to separate from the coast downstream Creus Cape for current intensities over the 0.3 m s^{-1} and as a consequence eddy shedding takes place at the lee of the cape. Simultaneously, as a consequence of NW winds, a downwelling develops over the shelf and when the wind stops, baroclinic processes take part on eddy growth. These baroclinic contributions are significant in conditions of strong stratification (i.e., the case of eddy EC0715, which reach the biggest dimensions and have the longest lifetime compared to the other eddies generated in the same area) although they are not key to eddy generation (i.e., eddy EC0413 generated on homogeneous conditions as a result of barotrophic processes).

4.2.2. Eddy Dynamics and Path

[35] In Table 2 we show Roussillon eddies characteristics at the Catalan Sea. These eddies are characterized by maxim diameters of 40 km and have a vertical extension between 70 m (eddy EC0627, generated in late June) and 100 m (eddy EC0715 generated on 15 July). The velocity associated with these eddies at 50 m is around 0.2–0.3 m s^{-1}. They are characterized by a low-density core since they incorporate the downwelled waters during their generation. After being generated over the shelf, these eddies are advected by the coastal current toward the slope and then they are advected by the NC toward the Catalan sea. Mean model eddies drifting velocities are around 6–7 km d^{-1} which is in accordance with the observations in the Catalan sea [*Rubio et al.*, 2005]. Moreover, as we have shown for eddy EC0715 in Figure 7, the hydrodynamic characteristics and 3-D structure of model Roussillon eddies are very similar to that of the eddy ET2001 observed in the Catalan Sea. These similarities suggest that ET2001 could have been generated at the lee of Creus Cape as a consequence of the coastal current separation. Taking into account the drift velocity and path of model eddies and the observations [*Rubio et al.*, 2005] the genesis of eddy ET2001, observed in the Catalan Sea around 25 September, could be related to an intense northwestern wind episode occurring between 4 and 11 September in the Gulf of Lions [see *Rubio et al.*, 2005, Figure 2]. In Figure 12 we show the evolution of the TS and relative vorticity vertical profiles of the three longest-lived eddies. These vertical profiles are extracted from 10 to 120 m at the center of each eddy (determined as explained in previous section). For clarity, we show the 2-day average vertical profiles for eddies EC0413 and EC0520 and the 5-day average vertical profiles for eddy EC0715. In all cases

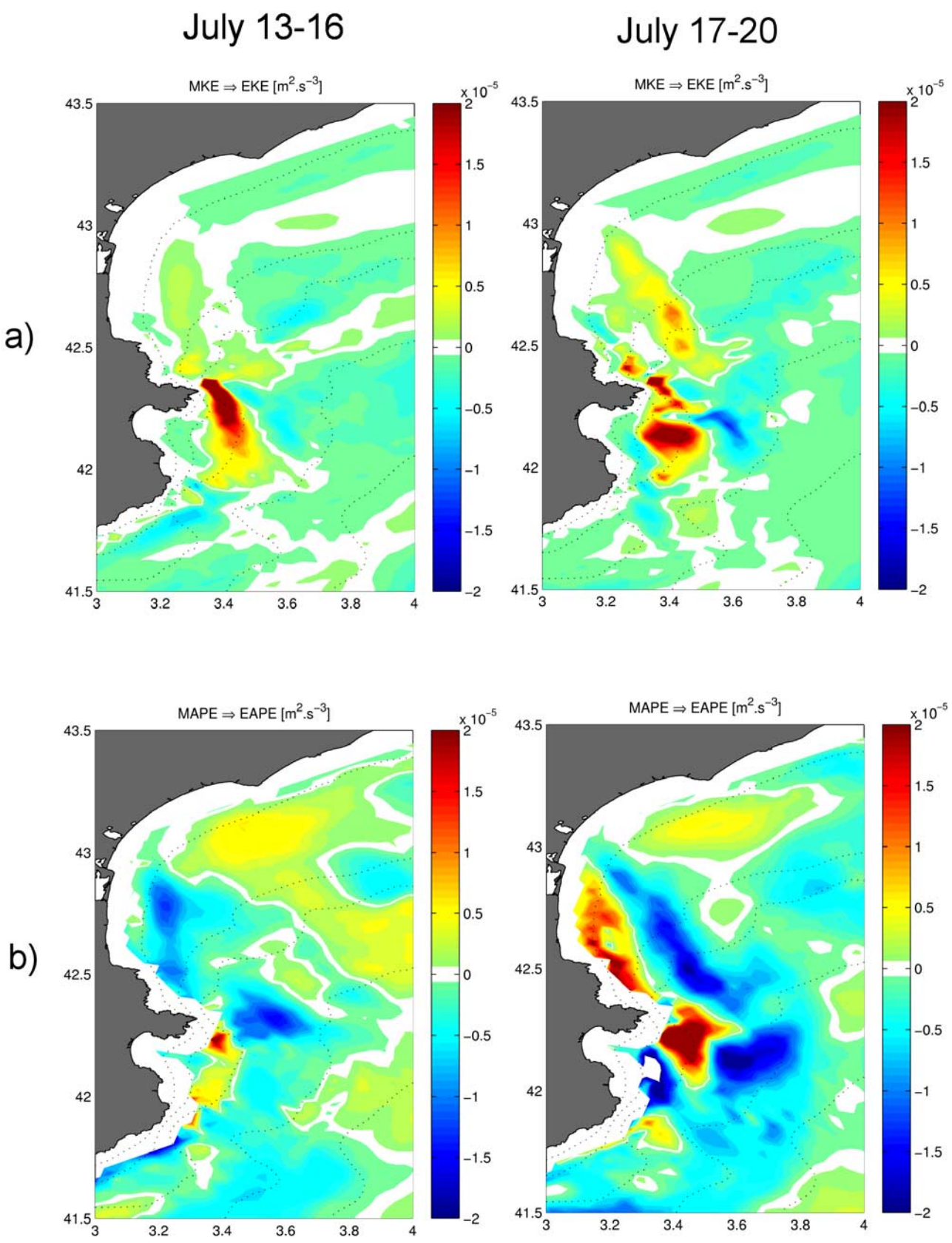

Figure 11. (a) MKE ⇒ EKE and (b) MAPE ⇒ EAPE transfers (m^2 s^{-3}) during the genesis of EC0715 Rousillon eddy. Transfers are computed between 10 and 100 m. Isobaths are at 10, 50, 100, 200, and 1000 m.

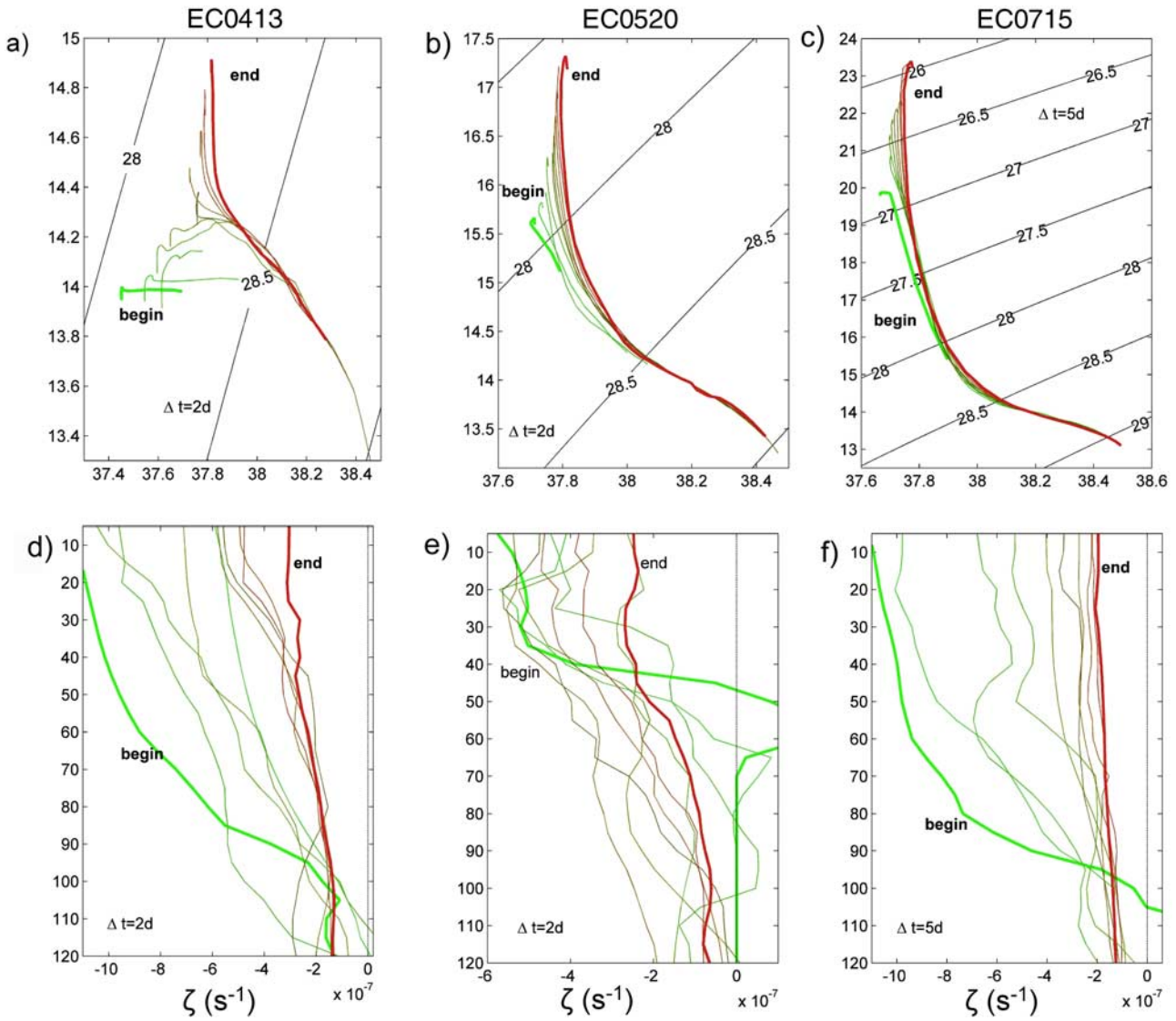

Figure 12. Time evolution of (a, b, c) TS and (d, e, f) relative vorticity profiles of Roussillon eddies EC0413 (Figures 12a and 12d), EC0520 (Figures 12b and 12e), and EC0715 (Figures 12c and 12f). Green profiles correspond to the beginning of eddy lives, and red profiles correspond to the end of eddy lives. Lines show the time evolution of the profile at 2-day interval for eddies EC0413 and EC0520 and at 5-day interval for eddy EC0715.

the variations in terms of salinity and temperature are significant in shallow and intermediate levels. Eddies become saltier and warmer as they incorporate the surrounding waters while they drift toward the Catalan Sea. At 50 m the variations in temperature from the beginning to the end of their lifetimes can reach the 3°C (case of EC0715). The increase in terms of salinity is around 0.1–0.3 psu. Concerning the relative vorticity profile, the three eddies present a similar evolution. During the first days the strong changes in vorticity reflect the variations of eddy sizes while the following days the attenuation in vorticity is associated with the eddy decay.

5. Summary and Conclusions

[36] In this work we have used a numerical regional model of the northwestern Mediterranean Sea to investigate the origin of Catalan Sea anticyclonic eddies. The validation of the simulations shows that the model is able to reproduce realistically the main characteristics of the ocean circulation of this region (i.e., the Northern Current path and variability, the wind-induced circulation over the shelf and the mesoscale variability). Numerical results have pointed out two areas of eddy generation in the NW Mediterranean: the Marseille coast and the southeast of the Roussillon coast. We have investigated the generation mechanism of model eddies and compared their characteristics to those of an anticyclonic eddy observed in the Catalan Sea in September 2001.

[37] Model results for Marseille eddies have shown that eddy generation in this area is linked to barotropic processes (horizontal shear instability) associated with the perturbation of the Northern Current by the bathymetry. In this area, a

major variation in the direction of the slope induces a separation of the Northern Current from the slope when current intensities exceed the 0.3 m s^{-1}. As a consequence of the flow separation, eddy shedding takes place over the slope (i.e., 600–1000 m isobaths). During their generation, eddies incorporate coastal low-density waters transported by the Northern Current. These eddies are characterized by diameters of 35 km, surface velocities around 0.2–0.3 m s^{-1} and southwestward drifting velocities around 7–9 km d^{-1}. Because of their barotropic origin, these eddies have a deep structure (300–400 m) which they maintain from the beginning to the end of their lifetime. This characteristic of Marseille model eddies is not in accordance with the observations in the Catalan Sea (the observed eddy had a vertical extent of ~100 m). Concerning their path, Marseille model eddies do not to reach the Catalan Sea as they vanish after 10 to 20 days of southwestward drift in the Gulf of Lions.

[38] Model results for the Roussillon eddies show that in this area the flow separation is also the mechanism responsible for eddy generation. In this case, flow separation and eddy shedding occur over the shelf downstream Creus Cape when the coastal current is intensified (current intensity over 0.3 m s^{-1}). The intensifications of the coastal current are linked to strong northwestern wind events in the Gulf of Lions and to intense downwelling over the shelf. Energy analysis suggests that eddies are generated by a combination of barotrophic and baroclinic processes: after the flow separation, eddies are enhanced by baroclinic processes linked to the relaxation of the downwelling density front. Model Roussillon eddies are advected by the coastal current toward the shelf break and then advected toward the Catalan Sea by the NC. Their drifting velocity is around 6 km d^{-1}, their surface velocity is about 0.2–0.3 m s^{-1} and their diameter ranges from 25 to 40 km. They are characterized by a low-density core as they incorporate downwelled waters during their generation. As they originate over the shelf, their vertical extent is limited (~100 m). These eddies have hydrodynamic characteristics and a 3-D structure similar to that of the eddy ET2001 observed in the Catalan Sea. These results combined to the analysis of observations in the Catalan Sea by *Rubio et al.* [2005] suggests that eddy ET2001 were generated at the downstream of the Creus Cape as result of flow separation triggered by an intense NW wind event in the Gulf of Lions. Then, eddy ET2001 could have been advected by the coastal and slope currents toward the Catalan Sea where it was observed around two weeks after it was generated.

[39] **Acknowledgments.** This work has been partially performed in the framework of the project "Génesis, evolución temporal, translación y efectos de remolinos de mesoescala sobre la plataforma continental Catalana (MAR1999–1010)" which has been funded by the Spanish Comisión Interministerial de Ciencia y Tecnología (CYCIT) and the project MFSTEP funded by the European Commission. The works of A. Rubio and G. Jordà were funded by a grant from the Spanish Ministerio de Educación, Cultura, y Deportes and by a grant of the Universitat Politècnica de Catalunya. The work of B. Barnier was supported by CNRS. The authors want to thank J. M. Molines and J. Puigdefàbregas for their support during the realization of this investigation and their many useful comments. Finally, the authors want to thank PRECARIOS, a postgraduates' organization whose dedication and effort contribute to improving young scientists' working conditions in Spain (www.precarios.org).

References

Albérola, C., C. Millot, and J. Font (1995), On the seasonal and mesoscale variability of the Northern Current during the PRIMO-0 experiment in the western Mediterranean Sea, *Oceanol. Acta*, *18*, 163–192.

Arakawa, A., and V. R. Lamb (1977), Computational design of the basic dynamical processes of the UCLA General Circulation Model, *Methods Comput. Phys.*, *17*, 174–267.

Arakawa, A., and M. J. Suarez (1983), Vertical differencing of the primitive equations in sigma coordinates, *Mon. Weather Rev.*, *111*, 34–45.

Arnau, P. A. (2000), Aspectos de la variabilidad de mesoescala de la circulación marina en la plataforma continental catalana, Ph.D. thesis, Universitat Politècnica de Catalunya, Barcelona, Spain.

Asselin, R. (1972), Frequency filters for time integrations, *Mon. Weather Rev.*, *100*, 487–490.

Astraldi, M., G. P. Gasparini, and G. M. R. Manzella (1990), Temporal variability of currents in the eastern Ligurian Sea, *J. Geophys. Res.*, *95*, 1515–1522.

Auclair, F., P. Marsaleix, and C. Estournel (2001), The penetration of the Northern Current over the Gulf of Lions (western Mediterranean Sea) as a downscaling problem, *Oceanol. Acta*, *24*, 529–544.

Beckers, J.-M. (1994), On destabilizing implicit factors in discrete advection-diffusion equations, *J. Comput. Phys.*, *111*, 260–265.

Böning, C. W., and R. G. Budich (1992), Eddy dynamics in a primitive equation model: Sensitivity to horizontal resolution and friction, *J. Phys. Oceanogr.*, *22*, 361–381.

Bougeault, P., and P. Lacarrére (1989), Parameterization of orography-induced turbulence in a meso-beta scale model, *Mon. Weather Rev.*, *117*, 1872–1890.

Conan, P., and C. Millot (1995), Variability of the Northern Current off Marseille, western Mediterranean Sea, from February to June 1992, *Oceanol. Acta*, *18*, 193–205.

Crépon, M., L. Wald, and M. Monget (1982), Low-frequency waves in the Ligurian Sea during December 1977, *J. Geophys. Res.*, *87*, 595–600.

Dufau-Julliand, C., P. Marsaleix, A. Petrenko, and I. Dekeyser (2004), Three-dimensional modeling of the Gulf of Lion's hydrodynamics (northwest Mediterranean) during January 1999 (MOOGLI3 Experiment) and late winter 1999: Western Mediterranean Intermediate Water's (WIW's) formation and its cascading over the shelf break, *J. Geophys. Res.*, *109*, C11002, doi:10.1029/2003JC002019.

Durrieu de Madron, X., O. Radakovitch, S. Heussner, M. D. Loye-Pilot, and A. Monaco (1999), Role of the climatological and current variability on the shelf-slope exchanges of particulate matter: Evidence from the Rhône continental margin (NW Mediterranean), *Deep Sea Res., Part I*, *46*, 1513–1538.

Estournel, C., X. Durrieu de Madron, P. Marsaleix, F. Auclair, C. Julliand, and R. Vehil (2003), Observation and modeling of the winter coastal oceanic circulation in the Gulf of Lions under wind conditions influenced by the continental orography (FETCH experiment), *J. Geophys. Res.*, *108*(C3), 8059, doi:10.1029/2001JC000825.

Flexas, M. M., X. Durrieu de Madron, M. A. Garcia, M. Canals, and P. Arnau (2002), Flow variability in the Gulf of Lions during the Mater HFF Experiment (March–May 1997), *J. Mar. Syst.*, *33–34*, 197–214.

Flexas, M. M., G. J. F. van Heijst, and R. R. Trieling (2005), The behavior of jet currents over a continental slope topography with a possible application to the Northern Current, *J. Phys. Oceanogr.*, *35*, 790–810.

Font, J., J. Salat, and J. Tintoré (1988), Permanent features of the circulation in the Catalan Sea, *Oceanol. Acta*, *9*, 51–57.

Font, J., E. Garca-Ladona, and E. G. Górriz (1995), The seasonality of mesoscale motion in the Northern Current of the western Mediterranean: Several years of evidence, *Oceanol. Acta*, *18*, 207–219.

Gaspar, P., Y. Gregoris, and J.-M. Lefevre (1990), A simple eddy kinetic energy model for simulations of the oceanic vertical mixing: Tests at station Papa and Long-Term Upper Ocean Study site, *J. Geophys. Res.*, *95*, 16,179–16,193.

Gatti, J., A. Petrenko, J. L. Devenon, Y. Leredde, and C. Ulses (2006), The Rhone River dilution zone present in the northeastern shelf of the Gulf of Lion in December 2003, *Cont. Shelf Res.*, *26*, 1794–1805.

Geernaert, G. L. (1990), Bulk parameterizations for the wind stress and heat fluxes, in *Current Theory, vol. 1, Surface Waves and Fluxes*, edited by G. L. Geernaert and W. J. Plant, pp. 91–172, Kluwer Acad., Dordrecht, Netherlands.

Holland, W. R. (1978), The role of mesoscale eddies in the general circulation of the ocean. Numerical experiments using a wind driven quasi-geostrophic model, *J. Phys. Oceanogr.*, *8*, 363–392.

Jordà, G. (2005), Towards data assimilation in the Catalan continental shelf. From data analysis to optimization methods, Ph.D. thesis, Universitat Politcnica de Catalunya, Barcelona, Spain.

La Violette, P. E., J. Tintoré, and J. Font (1990), The surface circulation of the Balearic Sea, *J. Geophys. Res.*, *95*, 1559–1568.

Marsaleix, P., F. Auclair, and C. Estournel (2006), Considerations on open boundary conditions for regional and coastal ocean models, *J. Atmos. Oceanic Technol.*, *23*, 1604–1613.

Masó, M., and J. Tintoré (1991), Variability of the shelf water off the northeast Spanish coast, *J. Mar. Syst.*, *1*, 441–450.

Millot, C. (1987), Circulation in the western Mediterranean Sea, *Oceanol. Acta*, *10*, 143–149.

Millot, C. (1990), The Gulf of Lions' hydrodynamics, *Cont. Shelf Res.*, *10*, 885–894.

Millot, C. (1999), Circulation in the western Mediterranean Sea, *J. Mar. Syst.*, *20*, 423–442.

Oey, L.-Y., and P. Chen (1992), A model simulation of circulation in the northeast Atlantic shelves and seas, *J. Geophys. Res.*, *97*, 20,087–20,115.

Pascual, A., B. Buongiorno Nardelli, G. Larnicol, M. Emelianov, and D. Gomis (2002), A case of an intense anticyclonic eddy in the Balearic Sea (western Mediterranean), *J. Geophys. Res.*, *107*(C11), 3183, doi:10.1029/2001JC000913.

Petrenko, A., Y. Leredde, and P. Marsaleix (2005), Circulation in a stratified and wind-forced Gulf of Lions, NW Mediterranean Sea: In-situ and modeling data, *Cont. Shelf Res.*, *25*, 7–27.

Petrenko, A., C. Dufau, and C. Estournel (2008), Barotropic eastward currents in the western Gulf of Lion, north-western Mediterranean Sea, during stratified conditions, *J. Mar. Syst.*, *74*, 406–428.

Pinardi, N., I. Allen, E. Demirov, P. De Mey, G. Korres, A. Lascaratos, P.-Y. Le Traon, C. Maillard, G. Manzella, and C. Tziavos (2003), The Mediterranean ocean forecasting system: First phase of implementation (1998–2001), *Ann. Geophys.*, *21*, 3–20.

Pinot, J.-M., J. L. Lopez-Jurado, and M. Riera (2002), The CANALES experiment (1996–1998): Interannual, seasonal and mesoscale variability of the circulation in the Balearic channels, *Prog. Oceanogr.*, *55*, 335–370.

Rubio, A., P. A. Arnau, M. Espino, M. Flexas, G. Jordà, J. Salat, J. Puigdefbregas, and A. Sánchez-Arcilla (2005), A field study of the behaviour of an anticyclonic eddy on the Catalan continental shelf (NW Mediterranean), *Prog. Oceanogr.*, *66*, 142–156.

Sabatés, A., and M. Masó (1992), Unusual larval fish distribution pattern in a coastal zone of the western Mediterranean, *Limnol. Oceanogr.*, *37*, 1252–1260.

Sammari, C., C. Millot, and L. Prieur (1995), Aspects of the seasonal and mesoscale variability of the Northern Current in the western Mediterranean Sea inferred from the PROLIG-2 and PROS-6 experiments, *Deep Sea Res., Part I*, *42*, 893–917.

Tintoré, J., D. P. Wang, and P. E. La Violette (1990), Eddies and thermohaline intrusions of the shelf/slope front off the northeast Spanish coast, *J. Geophys. Res.*, *95*, 1627–1633.

Ulses, C., C. Estournel, J. Bonnin, X. Durrieu de Madron, and P. Marsaleix (2008), Impact of storms and dense water cascading on shelf-slope exchanges in the Gulf of Lion (NW Mediterranean), *J. Geophys. Res.*, *113*, C02010, doi:10.1029/2006JC003795.

B. Barnier, LEGI, CNRS, 1025 Rue de la Piscine, B.P. 53, F-38041 Grenoble, France.

M. Espino, Laboratori d'Enginyeria Marítima, Universitat Politècnica de Catalunya, E-08034 Barcelona, Spain.

G. Jordà, IMEDEA, CSIC, UIB, E-07122 Palma de Mallorca, Spain.

P. Marsaleix, POC, 14 Avenue Edouard Belin, F-31400 Toulouse, France.

A. Rubio, AZTI-Tecnalia Marine Research Division, Herrera Kaia-Portualdea z/g, E-20110 Pasaia, Gipuzkoa, Spain. (arubio@azti.es)